HLA-E-restricted T cells primed by a modified HLA-B*57:01 restricted HIV-1 peptide suppress HIV-1 replication

Authors: Hong Sun[1,2,3*], Hongbing Yang[1, 2], Max Quastel[1], Simon Brackenridge[1], Wanlin He[1, 4], Anna E. Kliszczak[1], Margarida Rei[5], Persephone Borrow[1], Geraldine M Gillespie[1*], Andrew J McMichael[1,2,*]

Affiliations:

1. Centre for Immuno-Oncology, Nuffield Department of Clinical Medicine, University of Oxford, Old Road Campus, Oxford, UK
2. Chinese Academy of Medical Sciences Oxford Institute, Old Road Campus, Oxford
3. State Key Laboratory for Diagnosis and Treatment of Infectious Diseases, NHC Key Laboratory of AIDS Prevention and Treatment, National Clinical Research Center for Laboratory Medicine, The First Hospital of China Medical University, China Medical University, Shenyang, 110001, China
4. State Key Laboratory of Oral Diseases and National Center for Stomatology and National Clinical Research Center for Oral Diseases, West China Hospital of Stomatology, Sichuan University, Chengdu 610041, China
5. Gulbenkian Institute for Molecular Medicine, Lisbon, Portugal; Faculdade de Medicina, Universidade de Lisboa, Lisbon, Portugal.

Corresponding author: Andrew J McMichael, Centre for Immuno-Oncology, Old Road Campus Research Building, Oxford OX3 7DQ, UK .T: +44 7505 992806. E: andrew.mcmichael@ndm.ox.ac.uk

* Co-corresponding authors

COI: The authors have declared no conflict of interest exists.

Abstract:

HLA-E-restricted HIV-specific T cells offer exciting possibilities for immunotherapy. However, HLA-E binding peptides are rare. A recent study showed that in HLA-B*57:01 people living with HIV (PLWH), the peptide that dominates the T cell response, KAFSPEVIPMF (KF11), also stimulates HLA-E-restricted T cells, even though direct binding of this peptide to HLA-E could not be demonstrated. We therefore changed position 2 alanine for methionine in the peptide (referred to as KMF11) which greatly enhanced binding to HLA-E. This enabled the generation of stabilised HLA-E-KMF11 tetramers which were used to select and then grow specific T cell clones from T cells of HLA-B*57:01 negative blood donors primed with this peptide *in vitro*. Approximately 20% of these T cell clones reacted with HLA-E positive cells presenting the native KF11 peptide. Furthermore, these T cells inhibited replication of HIV-1 NL4-3 in CD4 T cells *in vitro*. Therefore, this native peptide can be presented by HLA-E to CD8 T cells, although priming *in vivo* may depend on cross reactivities to classical MHC Ia types. Nevertheless, such T cells could be exploitable for immunotherapy given the conservation of this HIV1 peptide epitope and the non-polymorphism in HLA-E.

One Sentence Summary:

A Modified HLA-B*57-Restricted KF11 Peptide Elicits HLA-E-Restricted T Cells that suppress HIV-1 infected cells

INTRODUCTION

As a non-classical HLA-Ib molecule, HLA-E is primarily notable for presenting the signal nonamer peptide, typically VMAPRTLVL (VL9), derived from conventional HLA-A and -C, plus some -B molecules, to the CD94/NKG2A/C receptor family expressed by NK cells and a subset of CD8 T cells. The interactions with the higher affinity inhibitory receptor NKG2A-CD94 and the lower affinity activating receptor NKG2C-CD94 play a crucial role in regulating innate immunity and maintaining immune homeostasis (1).

Recent increasing evidence suggests that HLA-E can play a secondary, and sometimes pivotal role in adaptive immunity, by presenting pathogen-derived peptides to CD8 T cells with potential to combat invasive infections. For instance, during *Mycobacterium tuberculosis* (Mtb) infection, CD8 T cells have been shown to recognise multiple pathogen-derived peptides presented by HLA-E, engaging in the immune response to Mtb infection and complementing conventional MHC-I responses (2-4). Similarly, HLA-E-restricted CD8 T cell responses specific to human cytomegalovirus (HCMV), hepatitis B virus (HBV), and SARS-CoV-2 have been described in viral infections, although usually at lower levels than classical T cell responses (5-7). Notably, unlike classical HLA-I molecules, HLA-E appears relatively resistant to virus mediated downregulation (7-9) and is also characterised by its limited genetic polymorphism and near-ubiquitous expression on the cell surface, albeit at low levels (10). These features make HLA-E an attractive target for CD8 T cell-mediated immune therapy across diverse infections.

Despite significant advancements in antiviral drug therapy, HIV/AIDS remains an incurable and life-threatening disease, with approximately 40 million people living with HIV, with 1.3 million new infections and 630,000 deaths reported in 2023 (UNAIDS data 2024). These statistics highlight the continuing need for inexpensive effective vaccines. The failure of drug therapy to eradicate the virus from people living with HIV-1 (PLWH) and highlights a need

for novel approaches, including immunotherapies, to achieve cures. Current vaccine efforts have predominantly focused on generating neutralising antibodies, but with increasing recognition that classical MHC-Ia–restricted T cell responses might also protect synergistically (11-13). The recent recognition that HLA-E can utilize an alternative antigen presentation pathway may provide new avenues for vaccine and therapeutic development (10). Remarkably, Hansen *et al*. demonstrated that a rhesus cytomegalovirus-vectored simian immunodeficiency virus (RhCMV/SIV strain 68-1) vaccine conferred protection to over 50% of rhesus macaques (RMs) against a highly pathogenic SIV challenge (14). This unprecedented level of protection was mediated by CD8 T cells recognizing SIV peptides presented by Mamu-E, the rhesus ortholog of HLA-E (15), providing a compelling rationale for leveraging HLA-E–restricted immunity in human vaccine strategies. Furthermore, the priming of MHC-E-restricted T cells can be achieved in other primate species, such as cynomolgus macaques, but does require species-matched CMV vectors (16).

We previously identified a HLA-E presented HIV Gag-derived peptide, RMYSPTSIL (RL9HIV), which is homologous to the SIV RMYNPTNIL (RL9SIV) previously identified as an immunodominant supertope in RMs immunized with the RhCMV-SIV vaccine (17). We demonstrated that RL9HIV could elicit HLA-E-restricted CD8 T cell responses capable of effectively controlling HIV infection in human CD4 T cells *in vitro* (17). In a later study, we identified a second HLA-E binding peptide in HIV-1 Rev (residues 100-108), that primed CD8 T cell clones that effectively suppressed HIV-1 replication, also *in vitr*o (18).

A recent study in HLA-B*57-positive PLWH identified CD8 T cell responses targeting the HIV-derived peptide KAFSPEVIPMF (KF11), which exhibited HLA-E restriction alongside its better-known HLA-B*57:01 restriction (19). The latter T cell response, alongside additional Gag specific T cell responses, is associated with control of HIV infection (20, 21). The KF11 specific HLA-E restricted T cell responses were detected *in vitro* using PBMCs derived from

HLA-B*57:01 PLWH co-cultured with genetically modified cell lines expressing specific HLA antigens. However, it was not possible to detect HLA-E-KF11 multimer binding and direct suppression of HIV-infected cells was not reported.

In this study, we explore HLA-E-restricted KF11 specific T cells further. To overcome the difficulty of demonstrating binding of the KF11 peptide to HLA-E, we substituted alanine (A) with methionine (M) at position 2 of KF11, a preferred anchor for HLA-E binding, that is deeply buried in the B pocket (22). This modification, referred to as the KMF11 peptide, significantly enhanced HLA-E binding, as demonstrated using multiple optimised HLA-E binding assays. The resulting KMF11/HLA-E tetramers were then used to select and expand KMF11-specific T cell clones after priming HLA-B*57:01-negative blood donors *in vitro*. Using antigen recognition and co-culture suppression assays, we observed that a number of T cell clones exhibited cross-reactivity with the native KF11 peptide and HLA-E-expressing antigen-presenting cells. Moreover, we identified four T cell receptors capable of inhibiting HIV-1 NL4-3 virus replication in primary CD4 T cells in vitro. These findings help pave the way towards novel vaccine and immunotherapy strategies aimed at targeting protective HLA-E–restricted CD8 T cell responses.

RESULTS

A mutant peptide of HIV Gag KF11 binds robustly to HLA-E molecule

An immunodominant HLA-B*57:01-restricted epitope, HIV $Gag_{162-172}$ KAFSPEVIPMF (KF11), was recently reported to also be presented by HLA-E*01:01 (19). In that study a genetically modified HLA-E-expressing 721.221 cell line was peptide pulsed and shown to be recognised by T cells from a subset of HIV-infected patients after co-culture. However, these HLA-E restricted T cell responses were predominantly detected in HLA-B*57 positive donors and it was not possible to visualise the T cells directly using KF11/HLA-E multimers. In order

to confirm and extend this finding, we first constructed single chain peptide-β2-microglobulin (β2m) -HLA-E (HLA-E*01:03) trimers (SCTs) and transfected them into HEK293T cells to assess whether KF11 could stabilise and enhance the cell surface expression of HLA-E detected by flow cytometry. The result showed that there was detectable binding of KF11 to HLA-E when stabilised in the SCT format (Fig.1A). We further evaluated the binding of KF11 to HLA-E*01:03 using differential scanning fluorimetry (DSF) which measures the melting temperature (T_m) of the peptide–HLA-E complex (pHLA-E). Since we can generate peptide-free HLA-E-β2m complexes (7), we were able to directly add excess peptide to these complexes. At a 10 Molar excess peptide concentration over HLA-E, the T_m of wild type KF11 bound to HLA-E was 43.7℃, which was only slightly higher than no rescue peptide control at 41.3℃. This indicates very weak binding to HLA-E. The positive finding with the SCT probably reflects the tethering of the peptide to the HLA-E molecule enabling peptide to rebind repeatedly after dissociation.

Given that the preferred amino acid anchor residue of HLA-E is a position 2 is Methionine (M), which is buried in the HLA class I B pocket (23), we substituted this amino acid for the position 2 alanine (A) in KF11 to give the peptide KMFSPEVIPMF (KMF11). This mutant peptide dramatically increased binding to HLA-E (T_m = 50.6℃), compared to the wild type KF11 peptide, and approached that of the dominant natural signal peptide VL9 (Fig.1B). A SCT assay incorporating the KMF11 peptide was subsequently performed and demonstrated that KMF11 stabilised HLA-E expression to a level comparable to that of the VL9 peptide (Fig.1C).

To further confirm these findings, we next tested binding of KF11 and KMF11 to HLA-E using a peptide-exchange enzyme-linked immunosorbent assay (ELISA) assay, as previously described, with the HLA class I signal peptide VL9 as a positive control, and with a no-rescue peptide control using the same concentration of DMSO as for the tested peptide (17, 24). Very weak binding of KF11 to HLA-E was observed, amounting to 9.2% of the VL9 signal, and

much lower than for the RL9HIV peptide (39.3%VL9). That level of binding of the RL9HIV peptide approached the minimum required for stable HLA-E tetramers and needs further stabilisation strategies to generate reliable reagents (17) (Fig.1D and E). In line with nDSF and SCT data, the mutant KMF11 dramatically increased binding, equating to 65.4% of the VL9 control (Fig.1E). The binding in the ELISA assay, measured as a percentage of VL9 binding, was highly correlated with the T_m result from the previous nDSF assay (Spearman correlation test R^2=1.00, p=0.0167, Fig.1F). Therefore, these data collectively indicate that the mutant peptide KMF11 binds strongly to HLA-E in comparison to the weakly binding wild type KF11 peptide.

As the side chain of the second amino acid in HLA-E binding peptides is buried in the B pocket of HLA-E (23) we argued that stabilised KMF11/HLA-E tetramers could be used to screen native KF11 specific TCRs with a good chance of detecting cross-reactive, KF11-specific T cells. This approach could offer a means of selecting these T cells for functional evaluation.

Generation of KMF11-specific HLA-E-restricted CD8 T cells from primed T cells from healthy donors

We next tested whether KF11-specific HLA-E-restricted CD8 T cells could be primed *in vitro* using the KMF11 peptide. We used peripheral blood mononuclear cells (PBMCs) from two HIV-1 negative, HLA-B*57:01 negative blood donors (Table S1). T cells were primed with KMF11 at a concentration of 50μM plus a cocktail of cytokines to activate and maintain the specific T cells in an autologous dendritic-cell (DC) differentiation T-cell priming assay *in vitro* (17, 25). Following 8 days of culture, we co-stained the cells with KMF11/HLA-E tetramers conjugated to allophycocyanin (APC) and phycoerythrin (PE) and gated on double positive cells to reduce the chances of isolating non-specific cells. We also excluded CD56

positive and CD94 positive CD8 T cells to avoid contamination by natural killer T cells (NK) or CD94/NKG2x expressing T cells. After 8 days of peptide priming, KMF11/HLA-E staining tetramer cells were detected at the frequency of 0.33% of CD8 T cells in donor 1 and 0.086% in donor 2 (Fig.2A).

In order to dissect the functionalities of KMF11-specific HLA-E-restricted CD8 T cells, we generated KMF11-specific CD8 T cell clones by FACS sorting tetramer+ CD8 T cells. Sorted cells were cultured at less than 0.4 cells per well in microwell plates with irradiated allogeneic feeder cells, phytohemagglutinin (PHA) and interleukin-2 (IL-2), as previously described (7). After 12 days, a total of 586 clones proliferated and KMF11/HLA-E tetramer staining identified KMF11 specific T cell clones C02, C06, C07, C10, C26 and C27, with distinct HLA-E tetramer staining patterns, as shown in Fig.2B, similar to our previous observation for SARS-CoV-2-specific T cell clones (7). The relatively low frequencies of tetramer staining of these cloned T cells, likely reflects the low affinity binding of their TCRs; similar to the patterns we have observed previously for other HLA-E restricted peptide epitopes (7, 17). Several clones gave no distinct tetramer staining, suggesting they are probably bystander activated T cells, and these served as negative controls (Fig.2C).

TCRs for all positive and negative HLA-E-KMF11 binding and non-binding clones, including those identified in Figure 2, were full-length sequenced using the SMART (Switching Mechanism at 5'end of RNA Template) and 5'RACE (5'Rapid Amplification of cDNA Ends) technique. Each clone expressed a single TCR β chain the near 100% sequence read identities confirmed that they were clonal expansions (Table 1). C07 expressed two TCR alpha chains.

The six clones C02, C06, C07, C10, C26 and C27 were further screened, using specific monoclonal antibodies for expression of co-receptors that could possibly account for HLA-E-KMF11 tetramer binding: NKG2A/C, ILT-2 and ILT-4. None of the clones expressed these receptors and none stained with HLA-E tetramers containing the VL9 peptide ligand of the NKG2A/C-CD94 receptors, indicating that KMF11 tetramer binding was specific to their TCRs (Fig.S1A and B).

Antigen recognition of KMF11-specific HLA-E-restricted CD8 T cells

For functional analysis of the CD8 clones, stable HLA-E-KF11 expression on antigen presenting cells (APCs) was required. The HLA-Ia-deficient K562 chronic myelogenous leukemia cell line was therefore transduced with the construct expressing a SCT of peptide-β2m-HLA-E*01:03 heavy chain, giving a relatively stable HLA-E-peptide complex. First, constructs with SCTs incorporating the KF11 and KMF11 peptides, β2m and the HLA-E*01:03 heavy chain were produced. A K562 line transduced with a construct expressing the SARS-CoV-2 peptide VMPLSAPTL (ECOV2P1), a strong binder to HLA-E (7) was also generated as a negative control. The sequences of the constructs were verified by Sanger sequencing. The different HLA-E-expressing K562 (K562E_KF11, K562E_KMF11 and K562E_ECOV2P1) cells were enriched by FACS sorting and further validated by HLA-E antibody (clone: 3D12) staining by flow cytometry (Fig.S2).

The functionality of the 6 KMF11-specific CD8 clones C02, C06, C07, C10, C26 and C27 was measured by assessing expression of TNFα, IFNγ, CD107a/b, the activation molecule CD137 and inhibitory molecules PD-1 and CTLA-4 following coculture with K562E cell lines expressing different HLA-E-peptide SCTs. K562 cells expressing HLA-E only served as the

mock control. Coculture with HLA-E expressing K562 and K562E_ECOV2 cells stimulated very low levels of activation or cytokine release in the T cell clones, while HLA-E-KF11 and HLA-E-KMF11 upregulated expression of the activation markers. (Fig.3A). The six selected T cell clones responded to both K562E_KMF11 and K562E_KF11 expressing APCs. Four of the clones showed elevated expression of CD137, whilst expression was low on C26 and clone C27 was negative. Clones C02, C07 and C10 produced relatively strong TNFα and IFNγ responses, although C02 gave similar responses to the ECOVP1 negative control. CD107a/b expression was strongest on clones C02, C07 and C27. All these clones expressed very low levels of PD-1 and CTLA-4 following stimulation. (Fig. 3B)

To summarise, the six clones gave low but significant responses when stimulated by K562 cells expressing single chain HLA-E KF11 and KMF11 trimers. There was no significant difference between KF11 and KMF11 although as noted above the tethering of peptide to HLA-E may mitigate the very low binding affinity of KF11 to HLA-E. Clones C07 and C02 gave the strongest responses, however, C02 showed cross reactivity to the ECOVP1 peptide-HLA-E complex specifically in relation to TNFα and IFNγ production.

Antigen-Specific Reduction of both KMF11- and KF11-SCT expressing K562E Cells by KMF11-specific HLA-E-restricted CD8 T cells

We then sought to determine whether the CD8 T cell clones could eliminate target K562E cells expressing KMF11, by establishing a flow-based assay where CD8 clones were co-cultured with K562E_SCT expressing target cells. In these co-cultures, the target K562E_KMF11 SCT- or the wild-type KF11 SCT-expressing target K562E_KF11 cells were pre-labelled with CellTrace CFSE and subsequently mixed with both K562E_Mtb44 SCT expressing cells (as a specificity control) and K562E (background control) cells at 1:1:1 ratio. If the clone is peptide specific, there should be fewer target cells remaining following co-

culture compared to K562E_Mtb44 SCT and K562E cells when compared to numbers of target cells in the incubations with the irrelevant CD8 clone control. Co-cultures were conducted at E:T ratios of 1:1 and 5:1 (and 20:1 in the K562E_KF11 SCT/CD8 cocultures) using the previously identified 6 responsive CD8 T cell clones (C02, C06, C07, C10, C26, C27) with two irrelevant ECOV2 CD8 T cell clones as controls. Following a 48-hour co-culture period, the cells were collected, and flow cytometry was performed to gate viable CD3, CD8 and double negative cells (K562E cells) for further quantification of the remaining percentage of K562E_KMF11 SCT- or KF11 SCT-expressing target cells (CFSE+) (Fig. S3; Shown for clone C26 in Fig. 4A and clone C06 in Fig. 4D respectively). The inhibitory effect of KMF11-specific HLA-E-restricted CD8 T cells, calculated as [1 - (% target cells with specific T clone / % target cells with irrelevant control T clone)] × 100], was used to test the specific reduction of target cells.

Initial co-culture experiments using K562E_KMF11 SCT target cells revealed a modest reduction in target cells in the presence of KMF11-specific CD8 clones at both the E:T ratios of 1:1 and 5:1, while irrelevant ECOV2 CD8 T cells showed minimal effect on target cell survival (Fig.4B). The reduction was dependent on a higher E:T ratio (*$p<0.05$, Wilcoxon signed rank test; Fig.4C). We next investigated whether KMF11-primed CD8 T cell clones could cross-recognise and inhibit target cells expressing the wild-type KF11 peptide. In the co-culture assay, we used K562E_KF11 SCT expressing target cells at E:T ratios of 1:1, 5:1, and 20:1 (Fig. S3; Fig. 4D). Following the 48-hour coculture, KMF11-specific CD8 T cell clones mediated a modest reduction of K562E_KF11 SCT positive target cells at a E:T 1:1 ratio (Fig.4E). The effect was enhanced at higher E:T ratios, with target cell percentages dropping to 8.9% (range: 4.7%-21.5%) at an E:T 20:1 ratio (Fig.4E). Remarkably, six specific CD8 clones (C10, C06, C02, C26, C07, C27) exhibited particularly potent and significant

incremental reduction of K562E_KF11 SCT positive cells across all three ratios (*p<0.05, **p<0.01, one-way ANOVA test followed by Tukey multiple comparisons test; Fig.4F). A subsequent time course assay performed at an E:T ratio of 20:1 for T cell clones C02, C06, C07, C10, C26 with 2 irrelevant CD8 clones as negative controls demonstrated the progressive reduction of K562E_KF11 SCT expressing cells by 5 KMF11-specific CD8 clones when tracked over timepoints of 6, 20, and 48 hours post-coculture. This progressive pattern confirmed time-dependent inhibition. (***p=0.0001, ****p<0.0001, one-way ANOVA with Tukey's multiple comparisons test; Fig.4G). Together, the data indicate that KMF11-specific HLA-E-restricted CD8 T cells could eliminate target cells presenting the wild-type KF11 antigen as a SCT in a dose-dependent and time-dependent manner, also suggesting that relatively high E:T ratios and longer time interactions may be important.

Antiviral effect of KMF11-specific TCR transduced primary CD8 cells

To assess whether the KMF11-specific TCRs confer antiviral recognition we transduced TCRs into fresh CD8 T cells. We chose the TCR alpha and beta chains sequences from four CD8 clones, C02, C10, C26 and C27 fused onto murine TCR constant regions (mTCRs). These products were introduced into lentiviral constructs, and subsequently transduced into activated primary CD8 T cells from healthy donors according to our established method (7). The TCRs transduced were KMF11-specific TCRs from clones C02, C10, C26, and C27 or an irrelevant HLA-E-restricted TCR specific for SARS-CoV-2 (1016 clone 1) which had demonstrated suppressive effect on infected Calu-3 cells in our previous study (7). As a further positive control we generated lentiviral expression constructs for the HLA-B*57:01 restricted KF11 specific TCRs from the Aga-a clone (20, 21) and also transduced this into fresh activated CD8 T cells. We demonstrated successful enrichment of mTCR positive CD8 T cells by FACS analysis, finding similar levels of TCR expression for each of the TCRs (Fig.5A).

We next questioned the capacity of primary CD8 T cells transduced with these TCRs to suppress HIV-1 replication *in vitro*. Replication-competent VSV-G pseudotyped HIV NL4-3 virus was used to infect previously activated, primary CD4 T cells from healthy donors. KMF11-specific or control TCR CD8 T cell transductants were then co-cultured with these HIV-infected primary CD4 T cells for 5 days at E:T ratios of 1:1 and 5:1. Using flow cytometry, the proportion of HIV-1 Gag positive cells in the viable CD3+CD8- T cell population was gated and analysed to reveal the suppressive effect at both E:T ratios for the TCRs (Fig.S4, Fig.5B). Notably, four KMF11-HLA-E specific TCR transductants (C02, C10, C26, C27) mediated significantly greater suppression of HIV-infected CD4 T cells when compared to the irrelevant, SARS-CoV-2 specific TCR control (Fig. 5C). At an E:T ratio of 1:1, the median suppression mediated by these transductants ranged from 30% to 45%, compared to 16% for the irrelevant controls. This enhanced suppression was more pronounced at an E:T ratio of 5:1, with medians of 75% to 91% versus 45% for the controls. (Fig.5C) The relatively high backgrounds with the control SARS-CoV-2 specific TCR transduced CD8 T cells likely reflected cytokine production resulting from their activation and expansion, likely causing non-specific killing of HIV-infected cells.

To benchmark the findings, we evaluated a canonical HLA-B*57:01-restricted TCR, AGA1, that we previously reported (26, 27). Using pseudotyped HIV NL4-3-infected CD4 T cells from three HLA-B*57:01-positive and three negative donors, we confirmed that AGA1 specifically targeted HLA-matched cells. This TCR exhibited significant antiviral activity against HLA-B*57:01-positive targets at E:T ratios of 1:1 and 5:1, despite some background at E:T 5:1, while showing no effect against HLA-B*57:01-negative cells, thereby confirming HLA restriction (Fig. 5D). The four HLA-E-restricted TCR transductants consistently suppressed target cells from all six donors (Fig. S5), confirming the reproducibility of the VSA.

The data illustrate the difference between classically HLA restricted T cell and the universality of HLA-E restricted T cells (Fig.5C). Collectively, the result indicates that KMF11-stimulated, KF11 reactive TCR CD8 transductants efficiently suppress HIV-infected primary CD4 T cells in a dose-dependent manner.

DISCUSSION

A comprehensive understanding of the priming mechanisms and functional roles of unconventional HLA-E–restricted CD8 T cells in HIV infection is crucial for developing novel immunotherapies and vaccine strategies. Having previously identified two HIV-derived HLA-E-restricted epitopes (17, 18), we set about investigating the anti-viral activity of the recently described HLA-E-restricted HIV $Gag_{162-172}$ (KAFSPEVIPMF, KF11) epitope (19). This natural B*57:01 restricted epitope is one of a number of gag-derived epitopes associated with sustained long-term non-progression in PLWH. Bansal *et al*. (19) found KF11 epitope specific HLA-E-restricted responses *in vivo* in PLWH who are HLA-B*57:01 positive. However, in their study HLA-E tetramers were not generated due to the instability of KF11 in complex with HLA-E. In our HLA-E binding assays where the peptide is added to peptide-free HLA-E-β2m complexes, KF11 bound very weakly to HLA-E (~10% the level of VL9 when tested by sandwich ELISA (24), a level of binding that does not enable production of stable HLA-E tetramers (17). In humans, HLA-E predominantly binds the canonical HLA-class I signal peptide VMAPRT(V/L)(L/V/I/F)L (VL9), but can also bind pathogen-derived peptides, including strong binders such as VMAPRTLIL from HCMV UL40 (28), RLPAKAPLL from *Mycobacteria tuberculosis* (3), VMPLSAPTL from SARS-CoV-2 NSP13 (7), and more modest binders Mtb14 (RMAATAQVL) from Mtb (29), RL9HIV (RMYSPTSIL) from HIV (23). All of these peptides have leucine or methionine at position 2 of the peptide, with the side chain anchored in the B pocket of HLA-E. We found that substituting methionine for alanine

at position 2 in KF11, giving the peptide termed KMF11 and dramatically enhancing binding to HLA-E. This was shown by nDSF measured melting temperature, which increased from 43^{o}C to 51^{o}C and separately by direct binding in a peptide-exchange ELISA (Figure 1). Thus, modifying the key anchor residue at position 2 stabilised peptide binding and facilitated successful tetramer generation. While similar strategies have been explored for MHC class I, *e.g.* C-trap linkage (17) or homo-homo cysteine modifications (30), our approach offers a more natural alternative that likely minimises structural alterations to the HLA-E-peptide interface.

The KMF11/HLA-E tetramers facilitated the isolation and growth of KMF11-specific T cell clones from *in vitro* KMF11 peptide-primed PBMCs from HLA-B*57:01-negative donors. Functional analyses revealed that a subset of these clones exhibited cross-reactivity with the native KF11 peptide when assessed using genetically modified K562 cells, that expressed the peptide bound to HLA-E in a SCT format, as antigen presenting cells (APCs). Crucially, four TCRs were identified with the ability to suppress HIV-1 NL4-3 replication in primary CD4 T cells cultures *in vitro,* indicating that this weak binding epitope is naturally presented by HLA-E during viral infection.

Since we confirmed that KF11 exhibits very weak binding to HLA-E, consistent with the findings of Bansal *et al*. (19), it seems likely that induction of KF11 specific HLA-E-restricted CD8 T cell responses arise in PLWH who are HLA-B*57:01-positive because of cross-reactivity mediated by T cells primed by HLA-B*57:01-KF11. Disease control in HIV infection has often been associated with distinct features of TCR clonotypes, including broader cross-reactivity to variant viral peptides and enhanced functional capabilities (31, 32). For HLA-B*57:01-restricted KF11 T cells, we and others have previously identified an immunodominant Vα5/Vβ19 TCR (AGA1) in HLA-B*57:01-positive PLWH, which sees this conserved KF11 peptide, and also cross-recognizes its rarer variants (26, 27, 33, 34). Furthermore, using a yeast display library, we recently demonstrated that this same TCR can

cross-react with microbe-derived peptides that only in part resemble the KF11 sequence (35), illustrating the cross reactivities of TCRs and highlighting a potential role for microbial antigens in shaping specific T cell immunity, and perhaps, the frequency of Vα5/Vβ19 usage. Thus, the initial immune response in HLA-B*57:01-positive individuals may primarily be directed against HLA-B*57:01-restricted KF11, with a subset of these T cell clones showing cross-reactivity to KF11 via HLA-E restriction. The rarity of naturally occurring KF11 specific T cell responses in PLWH who lack HLA-B*57:01 could reflect the more stringent requirements for T cell priming compared to targeting. Although enough KF11 binds to HLA-E to make a cell recognizable by T cells, as shown here in the HIV virus suppression assay, there may be insufficient surface expression to prime T cells *in vivo*. The cross-reaction hypothesis aligns with Bansal *et al.*'s observation of a shared group of β chain TCR usage between HLA-B*57- and HLA-E-restricted responses. A short sequence match was also seen here within the α chain CDR3s of clone 26 and the HLA-B*5701-KF11 specific Aga-1 TCR (20).

It is possible that very low-affinity TCRs that are close to, or even just below, the threshold of tetramer staining could still be functionally active *in vivo*. This phenomenon has been observed in cases where multimer staining fails to detect self-targeted T cell responses in cancer or autoimmune diseases (36-42), as well as in MHC-II-restricted antigen-specific CD4 T responses (43-45). In our study, HLA-E-restricted CD8 T cell clones exhibited only partial staining with HLA-E tetramers, a pattern also observed in our previous HIV-1 and COVID-19 studies (7, 17), as well as in other studies involving pathogen-specific or tumor-specific TCRs (7, 17, 46, 47). These findings are likely caused by the low affinity of TCRs and/or low density of TCR surface expression induced during long-term coculture (48). Detection methods with higher-order multimers (*e.g.*, spheromers, dextramers) (41, 49) might improve staining.

In our *in vitro* recognition and co-culture assays, the HLA-E-restricted KF11 specific clones demonstrated only a modest ability to secrete cytokines and to express activation markers upon antigen stimulation in commonly used short term assays. This has been observed previously for other HLA-E restricted T cell responses (7, 17) and likely reflects the cumulative effect of low affinity interactions between peptide-HLA-E and then with the TCRs. The latter is evidenced both by tetramer staining and the delayed viral suppression kinetics observed here, compared to what is typically observed for higher-affinity classical HLA-Ia-restricted TCRs. This aligns with findings demonstrating that CD8 T cells can mount detectable responses to low-affinity antigens (50). Similarly, low-affinity TCR interactions in tumor microenvironments have been shown to effectively mediate antitumor responses while preventing excessive T cell activation and subsequent exhaustion (51). As an index of T cell priming and activation, T cell responses may also be influenced by additional factors, such as co-receptor (CD8 or CD4) involvement and regulatory (stimulatory/inhibitory/adhesion) molecules stimulation. For example, Denkberg, G *et al.* found anti-CD8 antibodies could block the tetramer binding of a human tumor specific CD8 clone, indicating the important role of CD8 in pHLA-TCR interactions (52). Despite the suboptimal functional profile, the clones with cytotoxicity exhibited suppressive effect against KF11-expressing target cells over 48 hours, demonstrating their functional capacity for antigen-specific killing. Importantly, CD8 T cells transduced with TCRs from 4 of these clones also inhibited replication of HIV-1 NL4-3, which expresses only wild type KF11, in primary CD4 T cells *in vitro.* The CD4 T cell donors were both positive and negative for HLA-B*57:01. In contrast, the classical HLA-B*57:01-restricted TCR AGA1 only showed a suppressive effect on HIV infected CD4 cells from HLA-B*57:01-positive donors. Thus HLA-E-restricted T cells could contribute to viral control, in donors lacking HLA-B*57:01.

HLA-E is monomorphic in its peptide-binding cleft, giving it a potential advantage over highly polymorphic classical HLA-Ia molecules in vaccine design and other immunotherapeutic interventions. This is particularly important in the context of HIV-1 and other viral infections or tumor environments, where HLA-Ia molecules are often significantly downregulated to evade classical CD8 T cell responses, while HLA-E expression is typically upregulated, or remains undisrupted, to evade natural killer cell attack. In the context of cancer immunotherapy, there has also been recent interest in the role of low-avidity T cells, which have been shown to contribute to tumor control, while their high-avidity counterparts can become exhausted and lose cytotoxic functionality (46, 53). Collectively, these findings indicate that with low-avidity, functionally suppressive HLA-E-restricted T cells might provide an alternative or complementary strategy to conventional HLA-Ia-restricted immune responses, to broaden the efficacy of T cell-based therapies.

A primary limitation of our study is the lack of resolved crystal structures for the pHLA-E/TCR complex, which could reveal details of specific molecular interactions between the KF11/HLA-E complex and TCRs. While we have shown KMF11-specific TCRs can effectively suppress wild-type HIV-1 NL4-3 replication through KF11 recognition, future studies using epitope-mutant viruses and comprehensive peptide screening would be valuable to address whether there is cross-reactivity with other HIV peptides or the potential for mutant escape. Additionally, validation of these findings *in vivo* will be required. Such validation would be important to assess the killing capacity of these TCRs, particularly in tissue compartments where HLA-E is enriched and may be upregulated, and where classical HLA-Ia molecules are downregulated by the viral infection. Such models (54) also offer the advantage of conducting the experiments over extended time periods in contrast to the commonly used short term *in vitro* assays of T cell function.

In summary, our findings demonstrate that peptide modifications can enable priming of cross-reactive, functionally effective HLA-E restricted T cells. This study extends the avenue toward HLA-E-centric vaccines and immunotherapies, which may circumvent viral HLA-Ia downregulation as an immune evasion mechanism, while leveraging the broad global conservation of HLA-E, offering a strategy for treating persistent infections cause by HIV and other viruses.

MATERIALS AND METHODS:

Sex as a biological variable

Our study used the PBMCs obtained from leukapheresis cones from NHS Blood and Transplant, UK, including both sexes. Sex was not considered as a biological variable.

Cell lines and primary cells.

The MHC-I null K562 cell line was used as the APCs or target cells in the antigen recognition assay and coculture assays (17). These cells were genetically modified to express the HLA-E single-chain trimer (SCT), which incorporates peptide, HLA-E heavy chain, and β2m. The K562 cells transfected with HLA-E*01:03 (K562E) was kindly provided by Thorbald van Hall (Leiden University Medical Centre) (55). K562 cell line was obtained from the European Collection of Authenticated Cell Cultures (ECACC). Human embryonic kidney (HEK) 293T cells were obtained from the ECACC and were used for producing the lentivirus for cell transduction for TCRs and to generate HLA-E single chain trimer constructs. PBMCs from healthy male and female donors were isolated from leukapheresis cones obtained from NHS Blood and Transplant, UK and from HLA-typed PBMCs were obtained from Cambridge Bioscience Ltd. Both sources and obtained ethical approval and informed consent from the volunteer donors. Received blood cells were handled under the UK Human Tissue Authority

requirements. PBMCs were used to generate T cell clones and TCR transductants, to make CD4 T cells for HIV-1 infection in vitro and for supply of irradiated mixed lymphocyte feeder cells to expand T cell clones or transductants. $CD4^+$ or $CD8^+$ T cells were positively selected from PBMCs using magnetic beads according to the manufacturer's instructions.

Peptides

HLA-B leader sequence peptide VMAPRTVLL (VL9) and candidate peptides including KF11 (KAFSPEVIPMF), KMF11 (KMFSPEVIPMF), Mtb44 (RLPAKAPLL, RL9HIV (RMYSPTSIL) were synthesized by Genscript (>90% purity). A UV-labile HLA-B leader-based peptide (VMAPRTLVL) incorporating a 3-amino-3-(2-nitrophenyl)-propionic acid residue substitution at position 5 (J residue) was synthesised by Dris Elatmioui at Leiden University Medical Centre, The Netherlands. Lyophilised peptides were initially reconstituted to 200mM or 100mM in DMSO and aliquoted for cryopreservation at -80°C until further use.

Protein expression, purification and refolding

The details of HLA-E heavy-chain (HC) expression, including inclusion body preparation, solubilisation, refolding, and final purification performed according to protocols have been previously described (7, 15, 17, 23). Briefly, HLA-E*01:03 HC and β2m were cloned into expression vector, expressed in BL21 DE3pLysS competent Escherichia coli cells, and purified as inclusion bodies. After solubilisation in urea buffer, HLA-E*01:03 protein was refolded in Tris-arginine/glutathione redox buffer with peptide. Complexes were filtered, concentrated, and purified by Superdex S75 16/60 chromatography. The protein was then aliquoted for further analysis by SDS-PAGE electrophoresis to confirm the presence of HLA-E HC and β2m.

Differential scanning fluorimetry

The thermal stability of no-peptide and peptide-loaded HLA-E was determined by differential scanning fluorimetry (DSF) using Prometheus Panta instrumentation (Nanotemper).

In brief, 0.45 μg/μL of HLA-E was incubated with 10M excess peptide in a 20μL final volume of 50mM Tris pH 7, 150mM NaCl buffer for 30 minutes. Following incubation, approximately 20μL of individual samples were split between two Prometheus Panta nanoDSF Grade Standard Capillaries (Nanotemper, Munich, Germany) and transferred into a capillary sample holder. Excitation power was pre-adjusted to obtain a range between 8000 and 15,000 Raw Fluorescence Units for fluorescence emission detection at 330 nm and 350 nm. A thermal ramp of 1 °C/min from 20 °C to 95 °C was applied. Thermal melt data calling was automatically generated using PR.Panta Analysis, version 1.2 software.

Generation of antigen presenting cells

Single chain trimer constructs incorporating HLA-E *01:03 heavy chain, β2m light chain and different peptides (KF11, KMF11, ECOV2P1 and Mtb44) were genetically modified and confirmed as previously described. The lentivirus was generated with the above single chain trimer constructs, and then transduced into K562 cell lines to generate antigen presenting cells with different peptides for further functional assays (K562E_KF11, K562E_KMF11, K562E_ECOV2 and K562E_Mtb44).

HLA-E binding peptide-exchange ELISA assay

A highly sensitive HLA-E binding ELISA assay was conducted as previously described (17, 24). Briefly, refolded HLA-E proteins (0.5 μM) preloaded with a labile VL9 variant peptide (7MT2) were incubated overnight with excess tested peptides (100 μM) in a reaction buffer containing 400 mM L-arginine monohydrochloride, 100 mM Tris, 5 mM reduced glutathione, 0.5 mM oxidized glutathione, and 2 mM EDTA. The reaction mixture was then diluted 1:100 in phosphate-buffered saline (PBS) containing 2% bovine serum albumin (BSA), and 50 μL was added to ELISA plates pre-coated with 20 μg/mL anti-human HLA-E monoclonal antibody (catalog no. 3D12, BioLegend). After 1 hour of incubation, the plates

were washed with PBS containing 0.05% Tween-20 and treated with 2 μg/mL anti-human β2m horseradish peroxidase (HRP)-conjugated IgG antibodies (catalog no. PA1-29662, Invitrogen) for 30 minutes. Following additional wash steps, 50 μL of enhancement reagent (Dako EnVision, diluted in PBS/2% BSA with 1% normal mouse serum) was added to amplify the HRP signal. Subsequently, 100 μL of TMB substrate was applied for development, and the reaction was stopped using 100 μL of STOP Solution. Absorbance was measured at 450 nm using a FLUOstar OMEGA reader. Each peptide was tested in three independent peptide-exchange reactions, with duplicates from each reaction analysed. A VL9 positive control and a peptide-free no-rescue control to normalise background and calculate binding affinity as a percentage of VL9 binding. HLA-E binding rankings were determined using the formula: (average signal of the tested peptide − average DMSO signal) / (average VL9 signal − average DMSO signal).

HLA-E tetramer generation and staining on CD8 T cells

Biotinylated HLA-E*01:03 monomers subjected to UV peptide exchange were conjugated to streptavidin-bound PE or APC at a molar ratio of 4:1, following a previously described protocol (17). Additionally, conventional tetramers were prepared for VL9 (VMAPRTVLL). KMF11 primed CD8 T cells or CD8 clones were stained with UV-exchanged KMF11/HLA-E tetramers (0.5 μg per 1×10^6 cells) for 45 minutes at room temperature (RT) in the dark. After staining, cells were washed with PBS and subsequently labelled with Live/Dead Fixable Aqua dye and flow cytometry antibodies, including anti-CD3-APC-Cy7 (catalog no. 300318, BioLegend), anti-CD4-PerCP-Cy5.5 (catalog no. 344607, BioLegend), anti-CD8-BV421 (catalog no. 301036, BioLegend), anti-CD94-FITC (catalog no. 305504, BioLegend) and anti-CD56-BV510 (catalog no. 362534, BioLegend), for 20 minutes at RT in the dark. Following staining, cells were washed, fixed in 2% paraformaldehyde, and acquired using an LSR

Fortessa cytometer (BD Biosciences) or Attune NxT flow cytometer with CytKick Max (ThermoFisher). Data were analysed using FlowJo software v10.10.0 (Tree Star).

Induction of HLA-E-restricted CD8 response using DC differentiation T cell priming assay

PBMCs from 2 healthy donors were primed to induce the HLA-E-restricted CD8 T cell response using a modified dendritic cell (DC)-differentiation T-cell priming protocol reported previously. First, PBMCs were cultured at 1×10^7/mL in 6-well plates with KMF11 peptide (50μM) added on day 1 in AIM-V medium supplemented with GM-CSF and IL-4. A cocktail of cytokines (IL-1β, TNFα, prostaglandin E2, IL-7 and IL-15) were supplemented to differentiate and mature DC and expand T cells at day 1. On day 6, cells were collected and transfer into fresh complete media with IL-2, IL-7 and IL-15 to support T cell homeostasis. The flow staining with HLA-E tetramers and flow antibodies to surface markers was performed on day 8.

Live cell sorting and generation of HLA-E tetramer positive CD8 T cell clones

KMF11-primed CD8 T cells from healthy donors were first stained with KMF11/HLA-E tetramers conjugated to APC and PE for 45mins at RT in the dark. Following a PBS wash, cells were stained for 20 minutes at room temperature (RT) in the dark using Live/Dead Fixable Aqua, anti-CD3-APC-Cy7 (catalog no. 300318, BioLegend), anti-CD4-PerCP-Cy5.5 (catalog no. 344607, BioLegend), anti-CD8-BV421 (catalog no. 301036, BioLegend), anti-CD94-FITC (catalog no. 305504, BioLegend) and anti-CD56-BV510 (catalog no. 362534, BioLegend). $CD3^+CD4^-CD56^-CD94^-$CD8+Tetramer+ T cells were live-sorted using a FACSAria III sorter (BD Biosciences). Sorted cells were subsequently seeded into 384-well plates at a density of 0.4 cells per well, along with irradiated (45 Gy) allogeneic feeder cells (from three healthy donors, 2×10^6 cells/mL), and stimulated with PHA (1 μg/mL) and IL-2 (500 U/mL) in

complete media (CM). The CM consisted of RPMI 1640, 10% AB human serum (UK National Blood Service), 1% penicillin/streptomycin, 1% glutamine, 1% sodium pyruvate, 1% non-essential amino acids, and 0.1% beta-mercaptoethanol. After 12 days, T cell clones were further expanded using irradiated feeder cells with PHA and IL-2. Tetramer positivity was tested on expanded CD8 clones to confirm their specificity. Functional assessments of CD8 T cell clones were then conducted as described in subsequent sections.

TCR sequencing of HLA-E-restricted CD8 T cell clones

RNA was extracted from CD8 T cell clones using the RNeasy Plus Mini Kit (Qiagen). Approximately 100 ng of RNA was used to generate TCR libraries with the SMARTer Human TCR α/β Profiling Kit v2 (Takara Bio), following the manufacturer's protocol, which leverages SMART and 5' RACE technologies. Full-length TCR α and β chain sequences were obtained using a MiSeq Reagent Kit v3 (600-cycle) on an Illumina MiSeq platform. The raw BCL files were converted to FASTQ format using bcl2fastq (v2.20.0.422). Cogent™ NGS Immune Profiler Software (version 2.0, Takara Bio) was used to analyse the profile of full length TCR α and β chain sequences.

Functional assessment of KMF11-specific HLA-E-restricted CD8 T cells

To assess the functionalities of CD8 T cell clones, cells were rested in complete medium overnight before being cocultured with genetically modified K562 cell lines (null of classical HLA-I expression) including KMF11, KF11 or ECOV2P1 expressing HLA-E single chain trimer transduced K562 cell lines. HLA-E-expressing K562 cells were used as reference control. The coculture was conducted at a CD8: K562 ratio of 1:1 for 10 hours. For maximal functionality assessment, CD8 T cell clones were also treated independently with PMA/Ionomycin. Brefeldin A (5 μg/mL) and GolgiStop (5 μg/mL) were added after 1 hour of incubation, and anti-CD107a-BV421 and anti-CD107b-BV421 were included at the start of the

coculture. After incubation, cells were stained with Live/Dead Fixable Aqua and surface marker antibodies (anti-human CD3 and anti-human CD8) in PBS. Cells were then fixed and permeabilised using Cytofix/Cytoperm (BD Biosciences). Intracellular staining (ICS) was performed using fluorochrome-conjugated antibodies targeting TNFα (catalog no. 502909, BioLegend), IFNγ (catalog no. 502528, BioLegend), CD137 (catalog no. 309810, BioLegend), PD-1 (catalog no. 335714, BioLegend) and CTLA-4 (catalog no. 369610, BioLegend) in PermWash solution. Data acquisition was carried out on an Attune NxT flow cytometer with CytKick Max (ThermoFisher), and results were analysed using FlowJo v10.10.0 (Tree Star).

Inhibition effect of KMF11-specific HLA-E-restricted CD8 T clones assessed using coculture assay

CellTrace CFSE Cell Proliferation Kit (Invitrogen) prepared at a concentration of 0.8 μM in prewarmed PBS was used to trace the target cells. 5-10 × 10^6 K562E_KMF11 (or K562E_KF11) cells were washed with 10 mL PBS and then labelled with prewarmed CellTrace CFSE at 100 μL per 1 × 10^6 cells for 20 min at 37°C in the dark. CM media was then added for 5 min to quench the reaction. Following centrifugation at 350 × g for 5 min, the cells were resuspended and mixed with HLA-E expressing K562 (K562E) cells at the ratio of 1:1, and plated at 0.5 × 10^5 cells per well in duplicates in the 96-well plates. The concentration of CD8 clones or transductants were washed and adjusted to coculture with K562 target cells at different effector-to-target ratio (E:T) ratio of 1:1, 5:1 or 20:1 at 37°C in a 5%CO_2 incubator for 48 hours. The samples were washed with PBS and then stained with Live/Dead Fixable Aqua, anti-CD3-APC-Cy7 (catalog no. 300318, BioLegend), anti-CD8-BV421 (catalog no. 301036, BioLegend) for 15 min at room temperature. The cells were subsequently washed with PBS and fixed with 2% PFA for sample acquisition on the Attune NxT Flow Cytometer (ThermoFisher Scientific). Data were analysed using FlowJo software v10 (Tree Star). To assess the suppressive effect of CD8 cells, CD3 and CD8 negative, viable cells were gated for

further assessing the % of remaining CFSE positive K562E_KMF11 (or K562E_KF11) target cells. Percentages of inhibition of K562E_KMF11 (or K562E_KF11) target cells were calculated as: (percentage of CFSE positive cells in irrelevant clone control - percentage of CFSE positive cells in KMF11 (or KF11)-specific CD8 T cell clone condition) / percentage of CFSE positive cells in irrelevant clone control) × 100%.

TCR transduction into primary CD8 T cells

Primary CD8 TCR transductants were generated as previously described (7). Briefly, TCR alpha and beta VDJ regions were amplified and assembled into a pHR-SIN backbone with the murine TCR alpha and beta constant regions using the HiFi DNA Assembly cloning kit (NEB). Lentiviruses encoding HLA-E-restricted TCRs were generated by transfecting HEK293T cells with packaging plasmids pMD.G, pCMV-dR8.91 and pHR-SIN-TCR using Turbofectin (Origene). Primary $CD8^+$ T cells were isolated from PBMCs using CD8 MicroBeads (Miltenyi) and activated with CD3/CD28 Dynabeads (Thermo Fisher) in T cell medium supplemented with IL-2 and IL-15. Activated CD8 T cells were then transduced with freshly filtered lentiviruses. Transduction efficiency was evaluated on day 7 by flow cytometry using anti-mouse TCRβ antibody (clone no. H57-597, Biolegend). $TCR\beta^+$ $CD8^+$ T cells were isolated by cell sorting (BD Fusion) and expanded for a further 10-12 days before the downstream functional assessment of TCR transduced T cells.

Viral suppression assay

PBMCs were fresh separated from healthy donors and CD4 T cells were isolated from PBMCs using positive selection with anti-human CD4 magnetic beads, following the manufacturer's protocol (MACS, Miltenyi Biotech, Surrey, UK). CD4 T cells were then activated with anti-human CD3 monoclonal antibody at the concentration of 100 ng/ml (clone OKT3, invitrogen) in RPMI 1640 complete medium supplemented with 5% AB human serum,

1% Penicillin/Streptomycin and interleukin-2 (IL-2, 50 IU/ml) for 3 days. Replication-competent HIV NL4.3 virus pseudotyped with VSV-G was used in the infection. The activated CD4 T cells were infected with HIV-1 NL4.3 virus at a multiplicity of infection (MOI) of 0.01 via spinoculation for 2 hours at 27°C as previously described. After infection, HIV-infected CD4 T cells were washed and seeded in triplicate (1×10^5 cells/well) in complete medium supplemented with 5% AB human serum and IL-2 (50 IU/ml) in 96-well plates. Primary CD8 TCR transductants were added at effector-to-target (E: T) ratios of 1:1 and 5:1. An irrelevant TCR transductant (ECOV2) was included as control condition. After 5 days of co-culture, cells were collected and stained with Live/Dead Fixable Aqua dye and flow antibodies targeting surface markers including anti-CD3-APC-Cy7 (catalog no. 300318, BioLegend), anti-CD8-BV421 (catalog no. 301036, BioLegend), and anti-CD4-PerCP-Cy5.5 (catalog no. 344607, BioLegend), followed by permeabilisation using BD fix/perm solution for intracellular staining of HIV Gag p24 antigen (KC57-FITC, catalog no. 6604665, Beckman Coulter). Viral inhibition of HIV-infected cells was calculated as follows: Percentage of inhibition on HIV infection = (percentage of HIV Gag positive cells in CD4 T cells cultured alone - percentage of Gag positive cells in CD4 T cells cultured with CD8 TCR transductants) / percentage of Gag positive cells in CD4 T cells cultured alone) × 100. The viral suppression assay was performed with three replicates for each condition. Cells from each condition were pooled after culture to ensure > 10000 viable cells acquired for intracellular p24 staining and flow cytometry assessment.

Statistical analysis

Data analysis was performed, and graphs were generated using GraphPad Prism v10. Mann Whitney test or unpaired t test was adopted to compare difference between 2 groups where applicable. One-way ANOVA test followed by multiple comparisons test was used to compare the difference among more than two groups.

Study approval

Human blood mononuclear cells were obtained from blood donated to NHS Blood Transplant and from Cambridge Bioscience Ltd with ethical approval and informed consent. They were processed, cultured and cryopreserved in our laboratory under conditions licensed by the UK Human Tissue Authority (HTA).

Data availability: The raw data associated with the graphs in this paper are available on the linked MS Excel file. Any further details can be obtained by direct contact with the corresponding authors.

REFERENCES

1. Braud VM, et al. HLA-E binds to natural killer cell receptors CD94/NKG2A, B and C. *Nature.* 1998;391(6669):795–9.
2. Heinzel AS, et al. HLA-E-dependent presentation of Mtb-derived antigen to human CD8+ T cells. *J Exp Med.* 2002;196(11):1473–81.
3. Joosten SA, et al. Mycobacterium tuberculosis peptides presented by HLA-E molecules are targets for human CD8 T-cells with cytotoxic as well as regulatory activity. *PLoS Pathog.* 2010;6(2):e1000782.
4. van Meijgaarden KE, et al. Human CD8+ T-cells recognizing peptides from Mycobacterium tuberculosis (Mtb) presented by HLA-E have an unorthodox Th2-like, multifunctional, Mtb inhibitory phenotype and represent a novel human T-cell subset. *PLoS Pathog.* 2015;11(3):e1004671.
5. Murugesan G, et al. Viral sequence determines HLA-E-restricted T cell recognition of hepatitis B surface antigen. *Nat Commun.* 2024;15(1):10126.

6. Burwitz BJ, et al. MHC-E-Restricted CD8(+) T Cells Target Hepatitis B Virus-Infected Human Hepatocytes. *J Immunol.* 2020;204(8):2169–76.

7. Yang H, et al. HLA-E-restricted SARS-CoV-2-specific T cells from convalescent COVID-19 patients suppress virus replication despite HLA class Ia down-regulation. *Sci Immunol.* 2023;8(84):eabl8881.

8. Wang EC, et al. UL40-mediated NK evasion during productive infection with human cytomegalovirus. *Proc Natl Acad Sci U S A.* 2002;99(11):7570–5.

9. Papadopoulos AO, et al. Spatial regulation of CD8(+) T cells at the HLA-E-NKG2A axis drives HIV persistence in lymph node B cell follicles. *Cell Rep.* 2025;44(9):116181.

10. Früh K, et al. Targeting MHC-E as a new strategy for vaccines and immunotherapeutics. *Nat Rev Immunol.* 2025.

11. Arunachalam PS, et al. T cell-inducing vaccine durably prevents mucosal SHIV infection even with lower neutralizing antibody titers. *Nat Med.* 2020;26(6):932–40.

12. Borgo GM, and Rutishauser RL. Generating and measuring effective vaccine-elicited HIV-specific CD8 + T cell responses. *Curr Opin HIV AIDS.* 2023;18(6):331–41.

13. Maciel M, Jr., et al. Exploring synergies between B- and T-cell vaccine approaches to optimize immune responses against HIV-workshop report. *NPJ Vaccines.* 2024;9(1):39.

14. Hansen SG, et al. Immune clearance of highly pathogenic SIV infection. *Nature.* 2013;502(7469):100–4.

15. Hansen SG, et al. Broadly targeted $CD8^+$ T cell responses restricted by major histocompatibility complex E. *Science.* 2016;351(6274):714–20.

16. Malouli D, et al. Cytomegalovirus-vaccine-induced unconventional T cell priming and control of SIV replication is conserved between primate species. *Cell Host Microbe.* 2022;30(9):1207–18.e7.

17. Yang H, et al. HLA-E-restricted, Gag-specific CD8(+) T cells can suppress HIV-1 infection, offering vaccine opportunities. *Sci Immunol.* 2021;6(57).

18. Hwang JK, et al. HLA-E-VL9 antibodies enhance NK cell and CD8 (+) T cell cytotoxicity against HIV-infected CD4 (+) T cells. *bioRxiv.* 2025.

19. Bansal A, et al. HLA-E-restricted HIV-1-specific CD8+ T cell responses in natural infection. *J Clin Invest.* 2021;131(16).

20. Stewart-Jones GB, et al. Structures of three HIV-1 HLA-B*5703-peptide complexes and identification of related HLAs potentially associated with long-term nonprogression. *J Immunol.* 2005;175(4):2459–68.

21. Gillespie GM, et al. Cross-reactive cytotoxic T lymphocytes against a HIV-1 p24 epitope in slow progressors with B*57. *Aids.* 2002;16(7):961–72.

22. O'Callaghan CA, and Bell JI. Structure and function of the human MHC class Ib molecules HLA-E, HLA-F and HLA-G. *Immunol Rev.* 1998;163:129–38.

23. Walters LC, et al. Pathogen-derived HLA-E bound epitopes reveal broad primary anchor pocket tolerability and conformationally malleable peptide binding. *Nat Commun.* 2018;9(1):3137.

24. Walters LC, et al. Detailed and atypical HLA-E peptide binding motifs revealed by a novel peptide exchange binding assay. *Eur J Immunol.* 2020;50(12):2075–91.

25. Martinuzzi E, et al. acDCs enhance human antigen-specific T-cell responses. *Blood.* 2011;118(8):2128–37.

26. Stewart-Jones GB, et al. Structural features underlying T-cell receptor sensitivity to concealed MHC class I micropolymorphisms. *Proc Natl Acad Sci U S A.* 2012;109(50):E3483–92.

27. Gillespie GM, et al. Strong TCR conservation and altered T cell cross-reactivity characterize a B*57-restricted immune response in HIV-1 infection. *J Immunol.* 2006;177(6):3893–902.

28. Sullivan LC, et al. A conserved energetic footprint underpins recognition of human leukocyte antigen-E by two distinct αβ T cell receptors. *J Biol Chem.* 2017;292(51):21149–58.

29. Walters LC, et al. Primary and secondary functions of HLA-E are determined by stability and conformation of the peptide-bound complexes. *Cell Rep.* 2022;39(11):110959.

30. Barber C, et al. Structure-guided stabilization of pathogen-derived peptide-HLA-E complexes using non-natural amino acids conserves native TCR recognition. *Eur J Immunol.* 2022;52(4):618–32.

31. Kosmrlj A, et al. Effects of thymic selection of the T-cell repertoire on HLA class I-associated control of HIV infection. *Nature.* 2010;465(7296):350–4.

32. Chen H, et al. TCR clonotypes modulate the protective effect of HLA class I molecules in HIV-1 infection. *Nat Immunol.* 2012;13(7):691–700.

33. Yu XG, et al. Mutually exclusive T-cell receptor induction and differential susceptibility to human immunodeficiency virus type 1 mutational escape associated with a two-amino-acid difference between HLA class I subtypes. *J Virol.* 2007;81(4):1619–31.

34. Turnbull EL, et al. HIV-1 epitope-specific CD8+ T cell responses strongly associated with delayed disease progression cross-recognize epitope variants efficiently. *J Immunol.* 2006;176(10):6130–46.

35. Mendoza JL, et al. Interrogating the recognition landscape of a conserved HIV-specific TCR reveals distinct bacterial peptide cross-reactivity. *Elife.* 2020;9.

36. Aleksic M, et al. Different affinity windows for virus and cancer-specific T-cell receptors: implications for therapeutic strategies. *Eur J Immunol.* 2012;42(12):3174–9.

37. Bridgeman JS, et al. Structural and biophysical determinants of αβ T-cell antigen recognition. *Immunology.* 2012;135(1):9–18.

38. Wooldridge L, et al. Enhanced immunogenicity of CTL antigens through mutation of the CD8 binding MHC class I invariant region. *Eur J Immunol.* 2007;37(5):1323–33.

39. Wooldridge L, et al. Interaction between the CD8 coreceptor and major histocompatibility complex class I stabilizes T cell receptor-antigen complexes at the cell surface. *J Biol Chem.* 2005;280(30):27491–501.

40. Rius C, et al. Peptide-MHC Class I Tetramers Can Fail To Detect Relevant Functional T Cell Clonotypes and Underestimate Antigen-Reactive T Cell Populations. *J Immunol.* 2018;200(7):2263–79.

41. Dolton G, et al. Optimized Peptide-MHC Multimer Protocols for Detection and Isolation of Autoimmune T-Cells. *Front Immunol.* 2018;9:1378.

42. Cole DK, et al. Human TCR-binding affinity is governed by MHC class restriction. *J Immunol.* 2007;178(9):5727–34.

43. Sabatino JJ, Jr., et al. High prevalence of low affinity peptide-MHC II tetramer-negative effectors during polyclonal CD4+ T cell responses. *J Exp Med.* 2011;208(1):81–90.

44. Wooldridge L, et al. Tricks with tetramers: how to get the most from multimeric peptide-MHC. *Immunology.* 2009;126(2):147–64.

45. Massilamany C, et al. Detection of autoreactive CD4 T cells using major histocompatibility complex class II dextramers. *BMC Immunol.* 2011;12:40.

46. Singhaviranon S, et al. Low-avidity T cells drive endogenous tumor immunity in mice and humans. *Nat Immunol.* 2025;26(2):240–51.

47. Scriba TJ, et al. Ultrasensitive detection and phenotyping of CD4+ T cells with optimized HLA class II tetramer staining. *J Immunol.* 2005;175(10):6334–43.

48. Schrum AG, et al. Surface T-cell antigen receptor expression and availability for long-term antigenic signaling. *Immunol Rev.* 2003;196:7–24.

49. Gao F, et al. Spheromers reveal robust T cell responses to the Pfizer/BioNTech vaccine and attenuated peripheral CD8(+) T cell responses post SARS-CoV-2 infection. *Immunity.* 2023;56(4):864–78.e4.

50. Zehn D, et al. Complete but curtailed T-cell response to very low-affinity antigen. *Nature.* 2009;458(7235):211–4.

51. Hay ZLZ, et al. Low TCR Binding Strength Results in Increased Progenitor-like CD8+ Tumor-Infiltrating Lymphocytes. *Cancer Immunol Res.* 2023;11(5):570–82.

52. Denkberg G, et al. Critical role for CD8 in binding of MHC tetramers to TCR: CD8 antibodies block specific binding of human tumor-specific MHC-peptide tetramers to TCR. *J Immunol.* 2001;167(1):270–6.

53. Janicki CN, et al. Loss of CTL function among high-avidity tumor-specific CD8+ T cells following tumor infiltration. *Cancer Res.* 2008;68(8):2993–3000.

54. Wahl A, and Garcia JV. Humanized Mouse Systems to Study Viral Infection: A New Era in Immunology Research. *Annu Rev Immunol.* 2025;43(1):143–67.

55. Lampen MH, et al. Alternative peptide repertoire of HLA-E reveals a binding motif that is strikingly similar to HLA-A2. *Mol Immunol.* 2013;53(1-2):126–31.

AUTHOR CONTRIBUTIONS:

Study design, experiment performance, data analysis and manuscript writing: HS, HBY, GMG, AJMcM

VSV Pseudotyped virus and infection protocols: PB and AEK

HLA-E binding peptides prediction and testing: SB, MQ, GMG

SCT, DSF assays and protein production: SB, MQ, GMG

HLA-E peptide exchange assay: HS

CL3 laboratory experiments: HS, HBY, WLH

TCR cloning and transduction: HS, MR

ACKNOWLEDGEMENTS:

We are grateful to David Margolis MD (University of North Carolina-Chapel Hill), and Barton Haynes MD (Duke University) for many discussions throughout this project. We thank Thorbald van Hall (Leiden University Medical Centre) for generously providing the K562E cells.

This work is the result of NIH funding, in part, and is subject to the NIH Public Access Policy. Through acceptance of this federal funding, the NIH has been given a right to make the work publicly available in PubMed Central.

This work funded by the Chinese Academy of Medical Sciences (CAMS) Innovation Fund for Medical Science (CIFMS), China (2024-I2M-2-001-1) and by NIH: NIAID UM1 AI 164567-02, the Collaboratory of AIDS Researchers for Eradication (CARE). In addition, HS was

supported by China Scholarship Council (CSC)-COI MD/PhD High-level Medical Innovative Talent Scholarship, Prevention and Control of Emerging and Major Infectious Diseases-National Science and Technology Major Project (2025ZD01904400), National Natural Science Foundation of China (82472269) and the Non-profit Central Research Institute Fund of Chinese Academy of Medical Sciences (2023-PT320-01). WH was supported by National Natural Science Foundation of China (32500781).

Table 1. TCR usage of KMF11-specific HLA-E-restricted CD8 T cells

Clone	TRAV	TRAJ	CDR3_α	TCRα reads[B]	TRBV	TRBJ	CDR3_β	TCRβ reads[B]
C02	TRAV13-1	TRAJ12	CAASIMDSSYKLIF	100%	TRBV6-5	TRBJ2-7	CASSYSWTGYEQYF	100%
C06	TRAV3	TRAJ24	CAFSTDSWGKLQF	97%	TRBV20-1	TRBJ2-3	CSAIPPDTTRDTQYF	100%
C07[A]	TRAV12-1 TRAV8-3	TRAJ3 TRAJ3	CVVNIGASKIIF CAVGEDSSASKIIF	85% 15%	TRBV6-6	TRBJ1-6	CASSSAGVNSPLHF	100%
C10	TRAV1-2	TRAJ6	CAVRDRAGGSYIPTF	100%	TRBV18	TRBJ1-5	CASSPDGREPQHF	100%
C26	TRAV16	TRAJ13	CALLNSGGYQKVTF	100%	TRBV11-2	TRBJ2-6	CASREHNSGANVLTF	96%
C27	TRAV38-2DV8	TRAJ45	CAYQGGGADGLTF	100%	TRBV2	TRBJ1-6	CASSERWSSYNSPLHF	100%

[A]Clone C07 possessed 2 α chains. [B]Total reads from TCR sequencing were 55,907 (median, IQR: 32,939-95,353).

Figure Legends

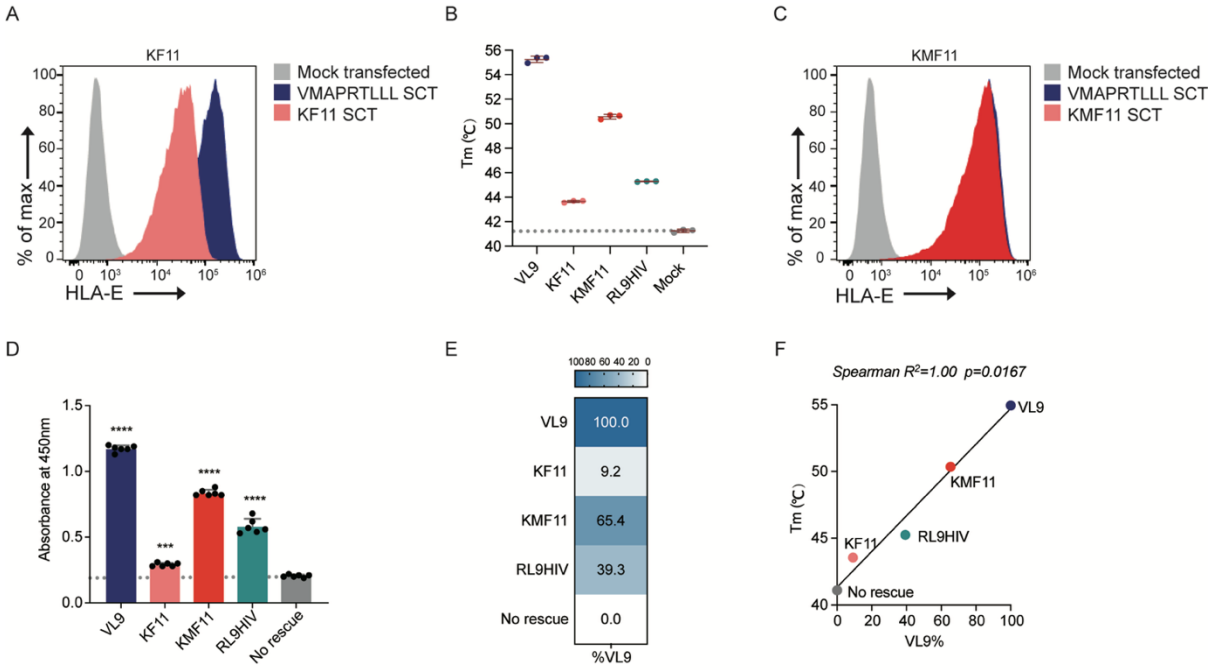

Fig. 1. Identification of a mutant peptide of HIV Gag-derived KF11 as an HLA-E binding peptide:

A, Binding of the HIV $Gag_{162-172}$ KAFSPEVIPMF (KF11) to HLA-E was evaluated using the single chain trimer (SCT) expression assay with VMAPRTLLL (VL9) included as a positive control.

B, The thermal melt (T_m) values of peptide-free HLA-E-β2m complexes incubated with 10M excess of KF11 and the peptide position 2 Ala to Met variant peptide (KMF11) was assessed by nano-differential scanning fluorography (nDSF). The positive control VL9 and mock no-peptide control was included for reference. The dot plot shows three biological replicates per peptide, presented as mean ± SD. Two technical replicates per peptide were measured per run.

C, Flow cytometry analysis of SCT expression demonstrated the binding potential of the mutant peptide KMF11 compared to the VL9 positive control.

D, HLA-E binding to KF11 and KMF11 were subsequently assessed using the peptide-exchange HLA-E peptide binding ELISA assay (24). The bar chart illustrates the raw absorbance value at 450nm (y axis) of tested peptides including KF11, KMF11, RL9HIV, positive control VL9 and no rescue negative control which included the same concentration of DMSO used for the test peptides (x axis). Error bars indicate Standard Deviation (SD). Statistical significance was assessed using one-way ANOVA with Dunnett's multiple comparisons test. ****p<0.0001. For ELISA-based screens, three independent peptide exchange reactions were performed per individual peptide (n=3), with 2 technical replicas per peptide tested.

E, The heatmap denotes the ranking of HLA-E binding strength data obtained using the sandwich ELISA assay, indicated as %VL9 binding.

F, Correlation of peptide-exchange HLA-E peptide binding ELISA reads and nDSF assay T_m data using the Spearman correlation method. VL9, blue; KF11, pink; KMF11, red; RL9HIV, green; no rescue, grey.

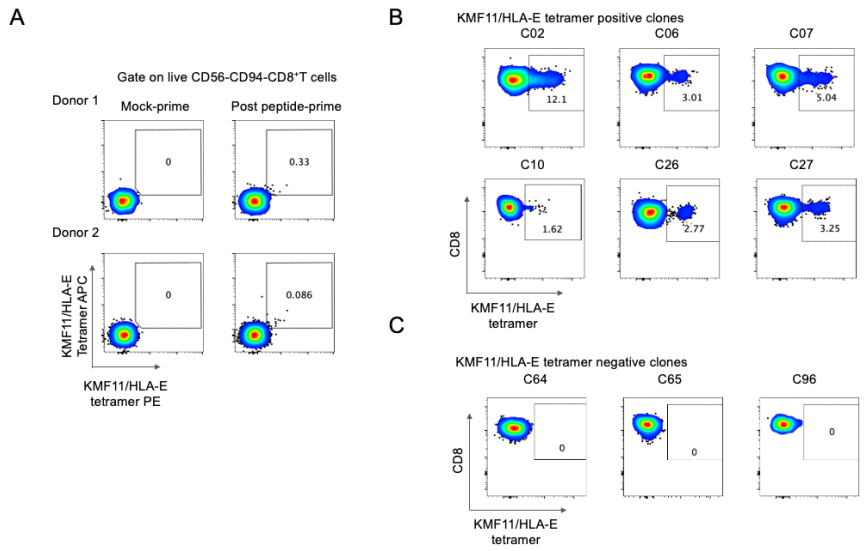

Fig. 2. Generation of KMF11-specific HLA-E restricted CD8 cell clones using an in vitro DC-differentiated T cell priming assay

A, KMF11-specific HLA-E-restricted CD8 T cells were primed from healthy donor-derived PBMCs using a DC-differentiation T-cell priming protocol (7, 25). Representative flow charts indicate the KMF11/HLA-E tetramer staining of primed T cells where tetramers were conjugated with APC or PE fluorescence, with mock-primed (left) and peptide-primed (right) conditions shown. Double tetramer+ gates were set on CD56 and CD94 double negative CD8 T cells.

B and C, KMF11/HLA-E dual tetramer+ CD8 T cells were sorted using a FACSAria sorter, then seeded at 0.4 cells per well culturing with irradiated feeder cells (45Gy) in CM with PHA/IL-2 for 12 days. CD8 T cell clones were identified if KMF11/HLA-E tetramer staining showed a distinct population (**B**), compared to other clones that showed no staining (examples in **C**).

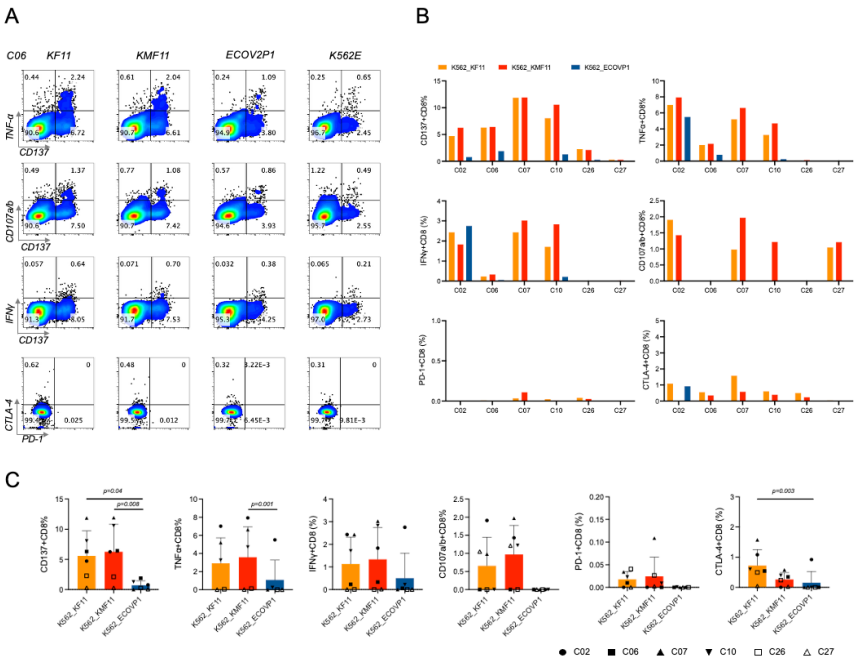

Fig 3. Functional characterisation of HLA-E restricted CD8 clones in response to antigen presenting cells.

A, Representative flow cytometry plots of KMF11 primed clone C06, demonstrating cytokine production (TNFα, IFNγ), activation (CD137, CD107a/b) and inhibitory marker expression (PD-1, CTLA-4) following coculture with K562E_KF11, K562E_KMF11 and K562E_ECOV2P1 following incubation for 10 hours. K562E cells were included as negative controls. Intracellular cytokine staining (ICS) of the above markers was performed following surface staining of Aqua viability dye, and anti-CD3, anti-CD8 antibodies. Percentages of CD8 T cells expressing the indicated markers are shown.

B, The expression of CD137, TNFα, IFNγ, CD107a/b, PD-1, and CTLA-4 for each CD8 clone in response to KF11, KMF11, and ECOV2-expressing K562E cells is shown. For normalization, the background of K562E control was subtracted from each antigen-specific condition. The y-axis denotes the percentage of effector marker positive CD8 T cells and the x-axis denotes individual CD8 T cell clones.

C, The expression of CD137, TNFα, IFNγ, CD107a/b, PD-1, and CTLA-4 expression in response to KF11, KMF11, and ECOV2P1-expressing K562E cells is noted in bar chart format. The Friedman test was used to test significance. P values are indicated.

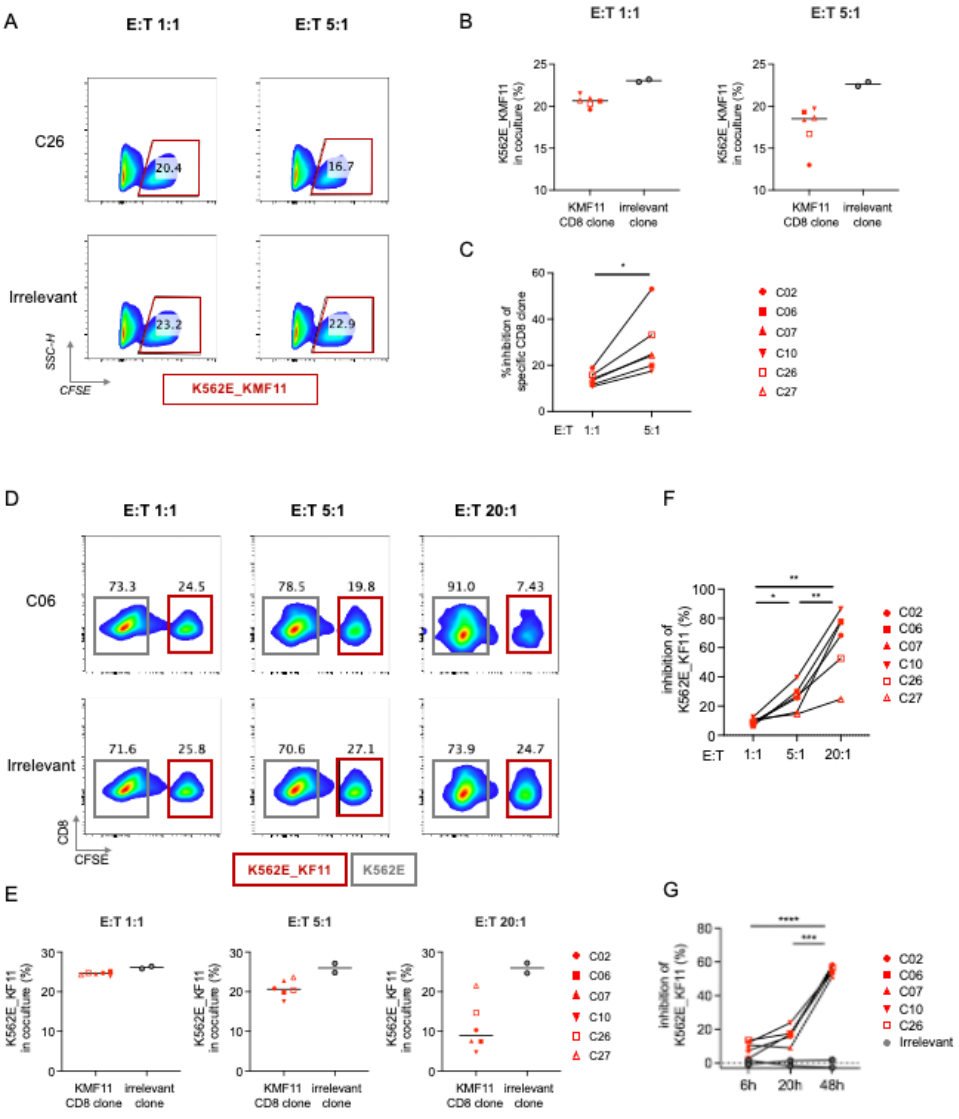

Fig. 4. KMF11-specific HLA-E-restricted CD8 T cells lyse antigen expressing K562E cells

A, K562E_KMF11 SCT cells, CellTrace CFSE labelled, were mixed with control K562E and K562E_Mtb44 SCT expressing cells at 1:1:1. These were cocultured with cloned KMF11-specific HLA-E-restricted CD8 T cells for 48 hours at E:T ratios of shown, in duplicate. Flow plots of clone C26 and a control clone are shown, gating on viable CD3-CD8- cells, quantifying K562E_KMF11 target cells remaining, boxed in red.

B, Percentage of CFSE positive K562E_KMF11 SCT cells following co-culture with KMF11-specific CD8 T cell clones (red symbols) or 2 irrelevant ECOV2 CD8 T cell clones (grey dots) at E:T 1:1 and 5:1.

C, Reduction of KMF11 SCT expressing cells cells by KMF11-specific, HLA-E-restricted CD8 T cells, using the formula: [1 - (% target cells with specific T clone / % target cells with irrelevant control T clone)] × 100 at E:T ratio of 5:1 compared to 1:1. Significance assessed using Wilcoxon signed rank test. *p<0.05. Each clone is denoted using different symbols. Two independent experiments were performed.

D, CellTrace CFSE labelled K562E_KF11 SCT cells were mixed with K562E cells and then cocultured with KMF11-specific HLA-E-restricted CD8 T cells for 48 hours, in duplicate. at E:T ratios shown. The percentage of K562_KF11 cells remaining are boxed in red.

E, The percentages of CFSE-positive K562E_KF11 SCT expressing cells following co-culture with KMF11-specific CD8 T cell clones (red symbols) or two irrelevant ECOV2 CD8 T cell clones (grey dots).
F, Increasing E:T ratios of 1:1 to 5:1, and 20:1 enhanced lysis of K562E-KF11 cells. Significance determined by one-way ANOVA test withTukey multiple comparisons test. *p<0.05, **p<0.01.
G Time-dependent inhibition of K562E_KF11 expressing cells by CD8 T clones. Two irrelevant T cell clones were negative controls
G Time-dependent inhibition of K562E_KF11 expressing cells by CD8 T clones. Two irrelevant T cell clones were negative controls. Significance tested by one-way ANOVA test with Tukey multiple comparisons test. ***p=0.0001, ****p<0.0001. Two independent experiments were performed.

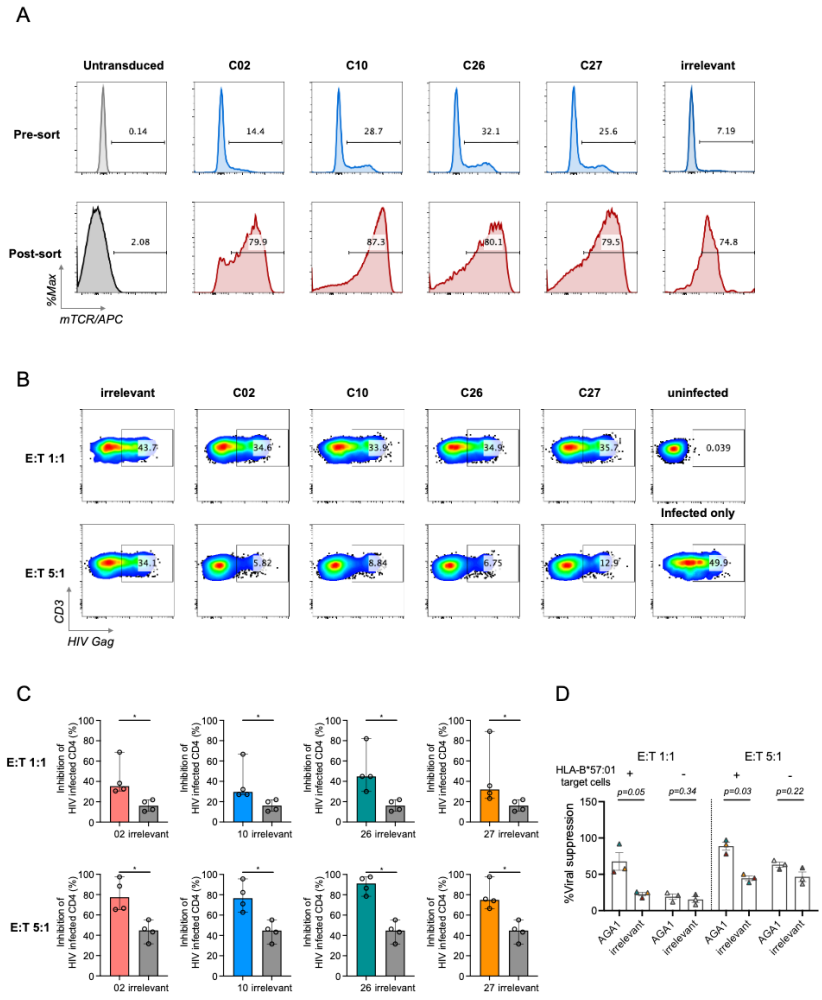

Fig. 5. Antiviral effect of KMF11-specific TCR CD8 T cell transductants against HIV-infected primary CD4 T cells in a viral suppression assay.

A, KMF11-specific TCRs (C02, C10, C26, C27) and an irrelevant HLA-E–restricted TCR specific for a SARS-CoV-2-derived peptide were transduced into primary CD8 T cells and then stained with anti-mouse Cβ antibody, anti-CD8/CD3, and LIVE/DEAD Fixable Aqua Dead Cell Stain Kit. Percentages of mTCR+ cells are indicated. Post enrichment staining of mTCR+CD8 T cell transductants for each TCR is shown. Untransduced CD8+ T cells were included as controls.

B, CD8 T cell transductants were cocultured with HIV-infected primary CD4 T cells at E:T ratios of 1:1 and 5:1 for 5 days. Intracellular HIV Gag staining (KC57-FITC) was performed following surface staining with anti-CD8/CD3/CD4, and LIVE/DEAD Fixable Aqua Dead Cell Stain Kit. The percentages of HIV Gag expression in HIV-infected primary CD3+CD8- T cells were assessed. Uninfected CD4 T cells and HIV-infected CD4 T cells without effectors were included as negative and positive controls, respectively.

C, The suppressive effect of KMF11-specific TCR transductants against HIV-infected $CD4^+$ T cells was assessed at E:T ratios of 1:1 and 5:1. Data are represented as the median with a 95% Confidence Interval (CI) from two independent experiments (n=4 donors). Statistical significance between KMF11 TCR transductants and irrelevant TCR controls was determined using the Mann Whitney test (*$p < 0.05$).

D, Suppression of HIV-infected $CD4^+$ T cells by HLA-B*57:01-restricted TCR transductants (AGA1) was evaluated at E:T ratios of 1:1 and 5:1. Data are represented as the mean ± Standard Error of the Mean (SEM) from two independent experiments. $CD4^+$ T cell targets were derived from six donors, comprising three HLA-B*57:01-positive and three HLA-B*57:01-negative individuals. Each donor is represented by a distinct colored circle. Statistical comparisons between AGA1 TCR transductants and irrelevant TCR controls were performed using a paired t-test.